Parallel Composition of Templates for Tail-Energized Planar Hopping

Avik De* Daniel E. Koditschek*

***Abstract*— We have built a 4DOF tailed monoped that hops along a boom permitting free sagittal plane motion. This underactuated platform is powered by a hip motor that adjusts leg touchdown angle in flight and balance in stance, along with a tail motor that adjusts body shape in flight and drives energy into the passive leg shank spring during stance. The motor control signals arise from the application in parallel of four simple, completely decoupled 1DOF feedback laws that provably stabilize in isolation four corresponding 1DOF abstract reference plants. Each of these abstract 1DOF closed loop dynamics represents some simple but crucial specific component of the locomotion task at hand. We present a partial proof of correctness for this parallel composition of "template" reference systems along with data from the physical platform suggesting these templates are "anchored" as evidenced by the correspondence of their characteristic motions with a suitably transformed image of traces from the physical platform.**

I. Introduction

The control of power-autonomous, dynamic legged robots that have a high number of degrees of freedom (DOF) is made difficult by a number of factors including (a) underactuation necessitated by power-density constraints, (b) the existence of significant inertial coupling and Coriolis forces that are hard or impossible to cancel, (c) variable ground affordance, (d) often hard-to-measure and necessarily rapid hybrid transitions. In the face of these challenges, some popular methods of controller design, such as feedback linearization [1]—which are "exact" in their domain of applicability but require extremely accurate qualitative and quantitative models—are hard to implement. Similarly, methods depending on local linearizations of the typically (highly) nonlinear dynamics found in dynamically dexterous locomotion and manipulation systems [2], [3] typically suffer from small basins of attraction [4] and high sensitivity to parameters.[1]

Observation (a) suggests that modularity of operation (i.e., wherein different combinations of actuators are used to effect distinctly different dynamical goals at different stages within the task cycle) will be a hallmark of practical locomotion platforms. Observations (b) and (c) imply that simpler, less exact but potentially more robust representations of the principal dynamical effects likely to prevail across a wide range of substrates may offer a tractable means of working with rather than fighting against, or learning exactly the highly varied dynamical details. Observation (d) implies that higher authority sensorimotor control activity ought to target continuous phases of the locomotion cycle, leaving the transition event interventions to more passive and mechanical sources of regulation [6]. In sum, these observations motivate the search for modular, reduced order representations of locomotion task constituents that are specialized to couple selected actuation affordances to particular DOFs at particular phases of the locomotion cycle. The value of such component task representatives remains hostage to the availability of methods for composing them in a stable manner.

This paper uses the design of a novel locomotion platform, the Penn Jerboa, Fig. 1, to put a slowly maturing formalism for the composition of such modules to a practical test. We adopt the template-anchor[2] framework [7] to represent this machine's 4DOF steady sagittal plane running as

Fig. 1. Snapshots from apex to apex of tail-energized planar hopping (§V) implemented on a new robot platform—the Penn Jerboa (§VI).

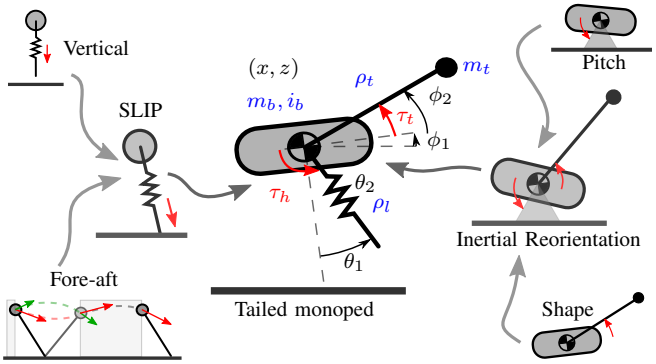

Fig. 2. Control of a hopping behavior expressed as a hierarchical composition of closed-loop templates. Notionally, the grey arrows represent directed template→anchor relations. **Center:** A model of the tailed monoped physical platform on which we implement tail-energized planar hopping, labeled with configuration variables (black), actuators (red), and model parameters (blue).

This paper uses the design of a novel locomotion platform, the Penn Jerboa, Fig. 1, to put a slowly maturing formalism for the composition of such modules to a practical test. We adopt the template-anchor[2] framework [7] to represent this machine's 4DOF steady sagittal plane running as

*Electrical and Systems Engineering, University of Pennsylvania, Philadelphia, PA, USA. {avik,kod}@seas.upenn.edu.

This work was supported in part by the ARL/GDRS RCTA project, Coop. Agreement #W911NF-1020016 and in part by NSF grant #1028237.

[1] In some robotics settings these disadvantages of the exact or local linearized control paradigm can be effectively remedied by recourse to parameter adaptation [5], but in our experience, such methods are too "laggy" to work in this hybrid dynamics domain with its intrinsically abrupt and rapidly switching characteristics.

[2] The template-anchor relation associates a pair of smooth vector fields, $f^{\mathsf{T}}, f^{\mathsf{A}}$ on a pair of smooth spaces, $\mathcal{T} \subset \mathcal{A}$ via the condition that $\mathcal{T}$ is an attracting invariant submanifold of the anchor field, f^{A}, whose restriction dynamics is conjugate to that of the template field, $f^{\mathsf{T}} \sim f^{\mathsf{A}}|_{\mathcal{T}}$ (where $\sim$ denotes equivalence up to smooth change of coordinates). In this paper, we are dealing with hybrid fields and flows for which the extended definition and its verification is a bit more intricate. Thus exceeding the scope and length constraints of the present paper, we will treat the hybrid template-anchor relation as an intuitive notion here.

the hierarchical composition of the low DOF constituents depicted in Fig. 2. At the leaves of this hierarchy tree, we introduce four different 1DOF templates that emerge from the decades old bioinspired running literature [3], [8], joined by a new arrival from recent work on bioinspired tails [9], [10]. We apply the four decoupled 1DOF control laws associated with these isolated "leaf" templates directly to the (highly dynamically coupled) physical platform and demonstrate empirically steady sagittal plane running (on a circular boom) whose body motions reveal, when viewed in the appropriate coordinates, Fig. 7, striking similarity to the corresponding isolated 1DOF constituents. We show (up to a still unproven technical conjecture) that the appropriate two pairs of these four 1DOF leaf templates are formally anchored by the two "interior" 2DOF templates depicted in Fig. 2, in the sense that the 1DOF systems define attracting invariant submanifolds of the 2DOF systems that exhibit conjugate restriction dynamics. We conjecture, as well, that the two interior nodes (the 2DOF templates) of the figure are in turn formally anchored by a physically realistic dynamical model of the closed loop Penn Jerboa in the sagittal plane. The data of Fig. 7 support this hypothesis, but we have not yet succeeded in completing the proof beyond the embedding and invariance properties.

Notwithstanding the specifics of our compositional approach to its control, we believe that the new physical platform is itself of independent interest by virtue of its added appendage (the "tail"), opening up a multiplicity of diverse uses for both of its two revolute actuators. Note again, however, this diversity of uses cannot be achieved without some recourse to behavioral modularity. In that light, we are particularly attracted by these simple low-DOF template controllers. In our experience, such constructions have the hope of succeeding in unstructured outdoor settings, since they build on the relatively robust template dynamics.

A. Relation to Prior Literature

This "compositional" method of controller synthesis was pioneered empirically by Raibert [11] for planar and 3D hopping machines, and we develop our planar hopping behavior by building up from those ideas. Our physical platform (Fig. 2 center) forgoes Raibert's prismatic shank actuator, and instead places that actuator in an inertial appendage. This motivates us to explore how tails can be "recycled" from their transitional agility duties [9], [10], now repurposed to substitute for Raibert's shank actuator and play the role of steady-state running energizer in the sagittal plane. Apart from their use in transitional maneuvers (inertial control in free-falling lizards [12] and robots [9], [10] or in turning lizards [13] and robots [14]) it has recently been discovered that kanagaroos do positive work with their tails in a quasistatic pentapedal gait [15]. In our implementation, the tail contributes the reorientation function in flight, and the energetic "pump" function in stance (albeit in a dynamic fashion). We are not aware of prior robotic locomotion work wherein a tail is used to help power the stance phase.

TABLE I
LIST OF SYMBOLS

$i \in \mathbb{Z}_2$	Hybrid mode, where 1 is stance, 2 is flight
$\mathcal{D}_i^\star$	Domain for template $\star$ in mode i
$f_i^\star : \mathcal{D}_i^\star \to T\mathcal{D}_i^\star$	Vector field in mode i
$r_i^\star : \partial\mathcal{D}_i^\star \to \mathcal{D}_{i+1}^\star$	Reset map from mode i to $i+1$
$F_i^\star : \mathcal{D}_i^\star \to \partial\mathcal{D}_i^\star$	Mode i flow evaluated at the next transition
$F^\star = F_2^\star \circ F_1^\star$	Return map at touchdown (TD) event
$p_i^\star(x,u)$	Plant to which we apply $u = g_i(x)$ to get $f_i^\star$
$I_d \in \mathbb{R}^{d\times d}$	Identity matrix of size d
$J = \left[\begin{smallmatrix} 0 & -1 \\ 1 & 0 \end{smallmatrix}\right]$	Planar skew-symmetric matrix
$\mathrm{R} : S^1 \to \mathrm{SO}(2)$	Map from angle to rotation matrix
$Tx = (x, \dot{x})$	Tangent vector associated with x
$D_x y$	Jacobian matrix $\partial y_i / \partial x_j$
$\kappa \in \mathbb{R}_+$	SLIP radial velocity gain (§III-B.2)
$h_\kappa \in \mathbb{R} \to \mathbb{R}_+$	Map from radial TD velocity to κ (§III-A.1)
$\gamma : \mathbb{R} \to S^1$	Fore-aft model stance sweep angle (§III-B.2)
$\beta : \mathbb{R} \to S^1$	Raibert touchdown angle function (7)
$h_{\mathrm{w}} : \mathbb{R}^2 \to \mathbb{R}^2$	Cartesian to Polar TD velocity (§III-C.2)

TABLE II
TEMPLATE CONTROLLERS

Tail energy pump	$g_1^{\mathsf{v}}(x) = k_t \cos(\angle x)$	(3)
Raibert stepping [11]	$g_2^{\mathsf{fa}}(\dot{x}) = \beta^*(\dot{x}) + k_p(\dot{x} - \dot{x}^*)$	(7)
Raibert pitch correction [11]	$g_1^{\mathsf{p}}(a_1, \dot{a}_1) = -k_g k a_1 - k_g \dot{a}_1$	(14)
Shape reorientation [10]	$g_2^{\mathsf{sh}}(a_2, \dot{a}_2) = -k_g k a_2 - k_g \dot{a}_2$	(14)

B. Contributions of the Paper

This paper contributes both to the theory and practice of dynamical legged locomotion. The principle theoretical contributions are: (i) a new (slightly simplified) further abstraction (§III-C) of the longstanding SLIP running model [3] as a formal cross-product of previously proposed vertical [16] and fore-aft [17] templates; (ii) a proof (modulo one remaining unproven conjecture) of local stability in this product dynamics of the parallel composition[3] of Raibert's [11] stepping controller (7) with our new energy pump (3); and (iii) a proof of local stability in the inertial reorientation model (13) of the parallel composition (14) of Raibert's [11] pitch stabilizer and the tail reorientation controller [10].

The principal empirical contributions of the paper are: (i) the design and implementation of a working tailed biped platform, the Penn Jerboa (Fig. 1); (ii) a physical demonstration of the (provably correct) oscillatory spring-energization scheme for vertical hopping; and (iii) experimental evidence supporting the hypothesis that our final parallel composition of the four isolated controllers does indeed anchor the corresponding templates in the Jerboa body (Fig. 7).

While the idea of parallel composition is appealing, the difficulty of such a composition arises from the natural transfer of energy between different compartments [18][4] in a mechanical system operating in a dynamical regime. In

[3] By this term we mean the application to the (coupled) plant $p^{\mathsf{s}}(x,u)$ of a decoupled control law, $u = g^{\mathsf{v}}(x_1) \times g^{\mathsf{fa}}(x_2)$.

[4] We use this term here to stand for subsystems (here, disjoint subsets of the physical degrees of freedom) that exchange a resource (here, energy).

our setting, some degree of coupling across compartments is crucial to the underlying design concept of driving the leg spring through torques generated "far away" in the tail. Thus, a naive approach of looking for exactly decoupled body dynamics is not fruitful[5]. Instead, we analyze stability properties of (hybrid) closed-loop templates–which are not specifically associated to any body–without paying attention to the input structure. In agreement with intuition, we find (§V-B) that minimization of cross-template transfer of energy–through either the flows or the reset maps–results in a successful composition.

II. Preliminaries: Organization and Notation

Table I contains a list of important symbols in this paper, including a set of symbols for describing hybrid dynamical systems. We adopt the modeling paradigm from Definition 1 in [19], representing a hybrid dynamical system by the tuple $(\mathcal{D}, f, r)$ as defined in Table I. We only consider two hybrid modes in this paper: ballistic flight, and a stance phase arising from a sticking contact at the "toe".

Superscripts on each of these symbols denote the *hybrid template* that it is a part of, e.g. $\star^{\mathsf{v}}$ for controlled vertical hopping (§III-A). The layout of the paper roughly reflects the template-anchor hierarchy depicted in Fig. 2. Namely, there are two intermediate 2DOF templates—the SLIP, s, and the inertial reorientation, a—-that comprise the tailed monoped, $\mathsf{tm} = \{\mathsf{s}, \mathsf{a}\}$. They, in turn, are comprised of the vertical, v, and fore-aft, fa, 1DOF templates, $\mathsf{s} = \{\mathsf{v}, \mathsf{fa}\}$, and respectively, the shape, sh, and pitch, p, 1DOF templates, $\mathsf{a} = \{\mathsf{sh}, \mathsf{p}\}$. We endow the 1DOF templates at the lowest level with an exemplar plant, with respect to which we will develop controllers for the four template plants, in isolation.

Sections III-IV present the 2DOF s, a templates that are directly anchored in the robot body (§V), and within them contain descriptions of the subtemplates (e.g. §III-A, III-B)—as simple exemplar 1DOF anchoring bodies and corresponding control laws—that comprise in isolation the constituent desired limiting behaviors that we seek to embody simultaneously in our physical system. Each of the template controllers in this suite is necessarily simple by dint of its origin as a feedback law for a highly abstract 1DOF task exemplar. We hypothesize that this combination of algorithmic simplicity and task specialization may lend robustness in the empirical setting since control policies are not sensitive to, and certainly avoid cancellation of, the various sources of crosstalk arising from their dynamical coupling in the anchoring body.

We emphasize that these coupling-naïve feedback laws (summarized in Table II) are simply "played back" (modulo scaling) in the 6DOF body (§V) with all its complicated true dynamical coupling. We show formally through various Propositions in this paper that nevertheless the stability of the templates and subtemplates persists through composition. Finally, we offer empirical data in §VI showing how this theory has been applied to the Jerboa robot.

[5]For instance, for hopping with the tailed monoped, the tail actuator and hip actuator seemingly work on differently "binned" tail and leg DOFs, but we energize the robot body with the tail through the leg spring.

III. The (2DOF) SLIP Template

A. Controlled Vertical Hopping (1DOF)

For a successful hopping behavior, energy must be periodically injected into the robot body to compensate for losses. We simplify the analysis here to a 1DOF vertically-constrained point-mass which can alternate between stance phase (during which the actuator has affordance) and a ballistic (passive) flight phase. It has been shown in the past empirically [11] and analytically [20] that an impulse at the bottom of stance can produce a stable limit cycle, in the presence of a spring for energy storage. In this paper, we consider a different strategy of an actuator forcing the damped spring by applying forces in a phase-locked manner. This choice of input representative is made with an eye toward using a tail actuator exerting inertial reaction forces on the spring (this model is formally instantiated §V). Intuitively, this can be thought of as negative damping [16] (effectively cancelling losses by physical damping).

We build upon the "linear spring" analysis in [20] for our vertical hopping exemplar body and closed-loop templates. We borrow the reparameterized form of the dynamics,

$$\ddot{\chi} + \omega^2(1+\sigma^2)\dot{\chi} + 2\omega\sigma\chi = \tau, \tag{1}$$

valid for the system being in an oscillatory regime. We make the following assumptions (to be used in Proposition 1):

Assumption 1 (Vertical hopper design)**.** *The parameters of the mass-spring-damper ensure (i) $\sigma^2 + \omega^2 = 1$ (such that $W := \left[\begin{smallmatrix} 1 & \sigma \\ 0 & \omega \end{smallmatrix}\right]$ has a simple inverse[6]) and (ii) $\omega > \sigma$.*

1) Oscillatory Spring Energization: W from Assumption 1 is a transformation to real-canonical form for the unforced system, i.e. if $x := W \left[\begin{smallmatrix} \chi \\ \dot{\chi} \end{smallmatrix}\right]$,

$$\dot{x} = p_1^{\mathsf{v}}(x, \tau) := (-\sigma I + \omega J)x + \left[\begin{smallmatrix} \sigma \\ \omega \end{smallmatrix}\right]\tau, \tag{2}$$

and the hybrid events of interest occur at $x_2 = 0$ (corresponding physically to the touchdown and liftoff events at $\chi = 0$). We choose the physically motivated control strategy

$$\tau := \tfrac{k_t x_1}{\|x\| + \varepsilon} \approx k_t \cos(\angle x), \tag{3}$$

where $\varepsilon > 0$ is a small saturation constant. It is clear in this form that the input is a fed-back version of the "phase" only. We obtain the closed-loop stance dynamics

$$\dot{x} = f_1^{\mathsf{v}}(x) := \left(-\sigma I + \omega J + \tfrac{k_t}{\|x\| + \varepsilon}\left[\begin{smallmatrix} \sigma \\ \omega \end{smallmatrix}\right] e_1^T\right) x. \tag{4}$$

Proposition 1 (Oscillatory energization stability)**.** *The vertical hopping template (4) has an attracting periodic orbit.*

Proof. Please see Appendix A. □

While this result guarantees periodic hopping behavior, we cannot yet preclude multiple limit cycles, some of which

[6]There is no loss of generality since this amounts to choosing a time scale, preserving all orbits and their limiting properties.

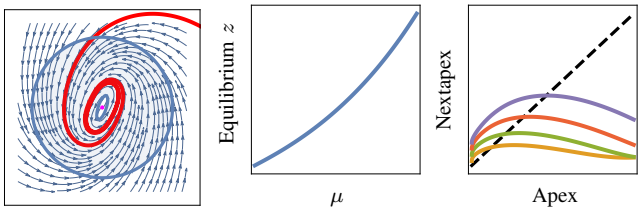

Fig. 3. **Left:** The vector field and an execution of (4), showing an annular trapping region. **Middle, Right:** Closed-loop simulation behavior of the hybrid vertical hopping system showing controllable hopping height and stable return maps.

may not be attracting. Encouraged by simulation results in Fig. 3, we make the following conjecture.

Conjecture 1. *The attracting limit cycle of (4) is unique and nondegenerate.*

As a corollary to Proposition 1, we know F_1^{v} (the vertical stance map, cf. Appendix B) has at least one asymptotically stable fixed point, $\dot{\chi}^*$, but we will now assume the non-degeneracy property of Conjecture 1, to assert as well that $-1 < DF_1^{\mathsf{v}} \mid_{\dot{\chi}^*} < 1$.

The ballistic flight portion of this simple model simply reverses the velocity,

$$F_2^{\mathsf{v}}(\dot{\chi}) := -\dot{\chi}. \tag{5}$$

Note that by symmetry (f_1^{v}, and consequently F_1^{v} are odd), $F_1^{\mathsf{v}} \circ F_1^{\mathsf{v}} = F_2^{\mathsf{v}} \circ F_1^{\mathsf{v}} \circ F_2^{\mathsf{v}} \circ F_1^{\mathsf{v}}$, i.e. the stability properties of the hybrid system are the same as that of the stance map as analyzed in Proposition 1.

Define

$$\kappa = h_\kappa(\dot{\chi}) := \frac{-F_1^{\mathsf{v}}(\dot{\chi})}{\dot{\chi}}, \tag{6}$$

the effective coefficient of restitution through stance, or the so-called "velocity gain" during SLIP stance [17]. Note that there is a unique fixed point, $\kappa^* = 1$, in these coordinates, which is necessary and sufficient for the smooth invertibility of h_κ, as can be seen by direct computation of its derivative.

Conjugating the touchdown velocity return map via this diffeomorphism, we can define a return map for κ, F^{v}.

Proposition 2 (Vertical stability)**.** *The velocity gain return map, F^{v}, has an asymptotically stable fixed point, $\kappa^* := 1$, assuming Conjecture 1 and, in fact, $DF^{\mathsf{v}} \mid_{\kappa=1} = -DF_1^{\mathsf{v}} \mid_{\dot{\chi}^*}$.*

Proof. This directly follows from the observation that κ and touchdown velocity are related by a diffeo, Proposition 1, and the simple form of F_2^{v} in (5). □

B. Controlled Fore-Aft Speed (1DOF)

Running and walking systems of a large variety from the sagittal or frontal plane resemble inverted pendula during stance [3]. Some prevalent robot control strategies for general fore-aft control and balance are ankle torques (if available), and stepping. We will focus on the second of these techniques, since our assumed model does not have an actuator at the toe. In prior literature, it has been shown that in SLIP, a fixed touchdown angle can admit a reasonable

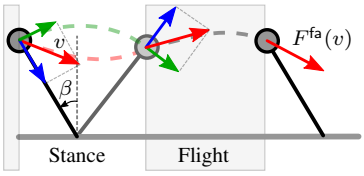

Fig. 4. A simple model for the 1DOF fore-aft dynamics in SLIP, closely related to BHop [17].

basin of stability around an emergent attracting steady-state velocity [21]. The capture point [22] and zero moment point [23] methods use a quasistatic heuristic which is related to these ideas, but are not explicitly designed to generalize to velocities other than zero. The empirical success of [11] is notable, and we attempt here to place it in the context of a model where its stability properties can be analyzed.

1) The Raibert Stepping Controller: In his classical empirical study, Raibert [11] inspired decades of subsequent experimentation and analysis by offering the following observations about the pendular stance phase in a running machine traveling at forward speed, $\dot{x}$, and stepping with a touchdown angle $\beta(\dot{x})$ (as in Fig. 4):

Assumption 2 (Raibert observations)**.** *(i) For each speed, $\dot{x}$, there is a neutral[7] touchdown angle, $\beta^*(\dot{x})$ (ii) this neutral angle is monotonic with speed, $D_{\dot{x}}\beta^* > 0$, and (iii) deviations from touchdown angle cause negative acceleration, i.e. $D_\beta(\dot{x}^+ - \dot{x}) \mid_{\beta=\beta^*} < 0$.*

Proposition 3 (Raibert stepping controller)**.** *Under assumptions 2(i-iii), the Raibert stepping controller,*

$$\beta : \dot{x} \mapsto \beta^*(\dot{x}) + k_p(\dot{x} - \dot{x}^*) \tag{7}$$

stabilizes the forward speed to $\dot{x}^*$.

Proof. Please see Appendix C. □

Surprisingly, notwithstanding the large literature arising from his pioneering ideas, to our knowledge, these simple observations represent the first stability analysis of any representation of Raibert's stepping controller. In order to establish a compositional view of SLIP, we will adopt a simple model of pendular stance that is in harmony with the Raibert assumptions, thereby automatically providing sufficient conditions for stability of the isolated fore-aft template closed-loop dynamics F^{fa} defined in (9)[8].

2) Modified BHop as a Fore-Aft Model: Building on existing SLIP literature [24], we make the following assumptions about pendular stance:

Assumption 3 (Pendular stance)**.** *During stance, (i) the effects of gravity are negligible compared to spring potential / damping forces, (ii) radial deflections are negligible,*

[7]In this context, "neutral" means $\dot{x}^+ = \dot{x}$, where $\dot{x}^+$ refers to the fore-aft speed at the subsequent touchdown event.

[8]Of course, the sufficiency of the Raibert stepping controller (7) for stability of the composed coupled systems is not automatic and represents a central contribution of the paper. This is established for the intermediate SLIP template, F^{s}, in Proposition 5.

(iii) time of stance is constant, and (iv) the angle swept by the leg admits a small-angle approximation.

Schwind [24] approximated that angular momentum about the toe is constant during stance, but we simplify further with the second assumption, and conclude that the angular velocity is roughly constant during stance. We adopt the third approximation from Raibert [11], and the last approximation is made for the ensuing analytical simplifications in §V-B, but we find empirically (§VI) that it is not critical in practice.

These assumptions lead directly to the construction of the following return map acting on touchdown velocity in Cartesian coordinates (cf. Fig. 4):

$$\begin{aligned} F^{\mathsf{s}}(v,\kappa) &= \left[\begin{smallmatrix}1 & \\ & -1\end{smallmatrix}\right] \mathrm{R}(-\gamma+\beta) \left[\begin{smallmatrix}1 & \\ & -\kappa\end{smallmatrix}\right] \mathrm{R}(-\beta) v \\ &= \mathrm{R}(\gamma-\beta) \left[\begin{smallmatrix}1 & \\ & \kappa\end{smallmatrix}\right] \mathrm{R}(-\beta) v, \end{aligned} \tag{8}$$

where κ (explicitly, the interaction from the radial component of SLIP) is taken to be a fixed parameter at this stage, $\gamma(v_1) \approx \frac{v_1 T_s}{\rho_l}$ is the angle swept by the leg over the course of stance and $\beta(v_1)$ is the leg touchdown angle (§III-B.1). This model is only a slight modification[9] of BHop [17].

This analytically tractable model (i) allows us to "separate" the dynamics in the radial compartment (encapsulated in κ) from the contributions of the fore-aft model itself, (ii) captures the exchange of vertical and horizontal kinetic energy through toe placement, and (iii) matches each of the empirically observed Raibert conditions (Fig. 5) as well as empirical data (Fig. 7), suggesting it is physically applicable and not just an analytical convenience.

In this Section, we restrict our attention to $\kappa = 1$, and generalize this to include the radial dynamics in §III. With this restriction,

$$F^{\mathsf{fa}}(v) := F^{\mathsf{s}}(v,1) = \mathrm{R}(\gamma - 2\beta) v, \tag{9}$$

While we choose to parameterize the return map as a function of $v \in \mathbb{R}^2$, it is really a 1D map (cf. Appendix D).

Proposition 4 (Fore-aft stability)**.** *MBHop with the Raibert controller presents a stable touchdown return map.*

Proof. Please see Appendix D. □

C. SLIP as a Parallel Composition

In order to anchor our 1DOF templates in the classical SLIP model (2DOF point mass with 2DOF springy leg), we simply "play back" our devised control schemes (Sections III-A and III-B). In the following subsections, we check that the closed-loop executions in the higher-DOF body still resemble a cross-product of our template behaviors. We emphasize that when moving to a more complex body, we do not add complexity to our controllers, rather, the closed-loop templates which we couple together are intrinsically amenable to parallel execution with minimal leakage of energy, by design. For instance, prior literature has observed a decomposition of SLIP dynamics into radial and tangential components, but to our knowledge there is no complete account of the stability of the parallelly composed (closed-loop) templates in these components.

[9]Specifically, the similarities are apparent between (8) and (19) of [17]. The slightly discrepancy should be attributed to our insistence on using the physical touchdown and sweep angles β and γ in the model, whereas the abstract parameter θ in [17] results in a more succinct form.

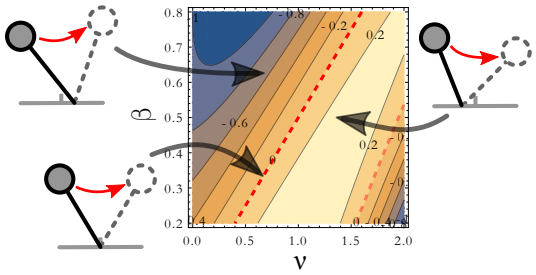

Fig. 5. A contour plot of the fore-aft acceleration $\dot{x}^+ - \dot{x}$ produced by the MBHop model for a range of fore-aft speed $\dot{x}$ and touchdown angle β. This plot depicts that (in a range around the neutral angle), this model captures all the conditions of Assumption 2.

1) Hybrid Dynamical Model of SLIP: We will construct our template plant model from [24]: a bead of mass 1 at (Cartesian) coordinates $(x^{\mathsf{s}}, z^{\mathsf{s}}) \in \mathbb{R}^2$, with a springy (Hooke's law spring constant k_s) massless leg of length[10] $\theta_2^{\mathsf{s}} \in \mathbb{R}_+$ (where $\mathbb{R}_+$ is restricted to *strictly* positive reals, and is open) and rest length ρ_l, at an angle of $\theta_1^{\mathsf{s}} \in S^1$ from vertical. Let $\mathbf{q}^{\mathsf{s}} := (\theta_1^{\mathsf{s}}, \theta_2^{\mathsf{s}}, x^{\mathsf{s}}, z^{\mathsf{s}})$. Using Assumption 3(iv) as a convenience (though that assumption is not required for this formulation), the touchdown and lift-off conditions can be specified in terms of the zeros of $\mathbf{a}^{\mathsf{s}} := z^{\mathsf{s}} - \rho_l$.

Define $\mathcal{Q}_i^{\mathsf{s}} := S^1 \times \mathbb{R}_+ \times \mathbb{R} \times \mathcal{I}_i$, where $\mathbb{R} = \mathcal{I}_1 \sqcup \mathcal{I}_2 := (-\infty, \rho_l] \sqcup (\rho_l, \infty)$. Then, $\mathcal{D}_i^{\mathsf{s}} := T\mathcal{Q}_i^{\mathsf{s}}$, and

$$f_1^{\mathsf{s}}(\mathbf{q}^{\mathsf{s}}, \dot{\mathbf{q}}^{\mathsf{s}}) := \left(\dot{\mathbf{q}}^{\mathsf{s}}, \begin{bmatrix} -\frac{2\dot{\theta}_1^{\mathsf{s}} \dot{\theta}_2^{\mathsf{s}}}{\theta_2^{\mathsf{s}}} \\ \theta_2^{\mathsf{s}} \dot{\theta}_1^{\mathsf{s}\,2} + k_s(\rho_l - \theta_2^{\mathsf{s}}) \\ \star \end{bmatrix} \right), \tag{10}$$

$$f_2^{\mathsf{s}}(\mathbf{q}^{\mathsf{s}}, \dot{\mathbf{q}}^{\mathsf{s}}) := \left(\dot{\mathbf{q}}^{\mathsf{s}}, \begin{bmatrix} \star \\ 0 \\ -g \end{bmatrix} \right), \tag{11}$$

where the unspecified components are (i) the mass-center dynamics which are constrained by $\left[\begin{smallmatrix} x^{\mathsf{s}} \\ z^{\mathsf{s}} \end{smallmatrix}\right] = \theta_2^{\mathsf{s}} \left[\begin{smallmatrix} -\sin\theta_1^{\mathsf{s}} \\ \cos\theta_1^{\mathsf{s}} \end{smallmatrix}\right]$ in (10), and (ii) the degenerate massless leg dynamics in (11). Please see Appendix E for more details.

2) Anchoring the 1DOF Templates: Consequent upon the above model—where each hybrid mode is dynamically 2DOF—SLIP is a 4D dynamical system (one parameterization being (x, z, v), where $v \in \mathbb{R}^2$ is the touchdown velocity, and $(x, z) \in \mathbb{R}^2$ is the Cartesian location of the point mass at touchdown). The efficacy of our 2D return map analysis is established by arguments similar to those of [26]: the Poincare section $z^{\mathrm{TD}} = \rho_l \cos\beta(v)$ eliminates one dimension, and the equivariance of the dynamics with x eliminates another.

We first observe that our MBHop model of §III-B.2 still represents the pendular stance correctly under Assumption 3. However, κ is not a fixed parameter, but evolves according to dynamics similar to F^{κ} in Proposition 2.

[10]We use θ for leg "joints" to be consistent with [25].

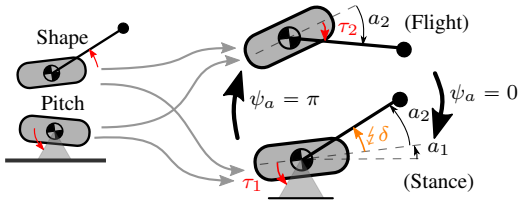

Fig. 6. A hybrid 2DOF inertial reorientation template with two segments pinned at the CoM and no gravity. **Left:** the net angular momentum of the system is constant. **Right:** the system can correct the net angular momentum using reaction torques on the main body segment, but the tail DOF is subject to an unmodeled disturbance $\lightning$, or δ in (13).

We observe from (7) and (8) that the embedded ($\kappa = 1, v = v^*$) submanifold is invariant, and show in Proposition 5 that is also attracting.

Let us define $h_{\mathrm{w}} : \mathbb{R}^2 \to \mathbb{R}^2$ as

$$w = h_{\mathrm{w}}(v) := \mathrm{R}(-\beta(v))v. \tag{12}$$

This mapping is a local diffeomorphism (Appendix F), and the vector w gives a tangential/radial decomposition of v (i.e. polar with respect to the leg angle).

Additionally, using (6), we can "recover" the κ-dynamics in the coupled system: $\kappa = h_\kappa(w_2)$. We prefer the redundant (v, κ) parameterization because of analytical tractability.

Proposition 5 (Stability of SLIP as a composition)**.** *For (i) stable vertical hopping with $-1+\varepsilon_{\mathrm{r}} < -DF_1^{\mathrm{v}}\,|_* < 1-\varepsilon_{\mathrm{r}}$, (ii) sufficiently*[11] *small k_p in the Raibert contoller, parallel composition of the radial and fore-aft templates results in a locally stable 2D return map, F^{s}.*

Proof. Please see Appendix G. □

IV. Hybrid Inertial Reorientation (2DOF)

Our decision to energize the hopping behavior with a tail leaves introduces a new actuated DOF whose tight dynamical coupling to both the mass center and the body orientation dynamics requires its careful control throughout the locomotion cycle. Recent literature [10] has seen the development of a 1DOF "inertial reorientation" template for correcting the "shape" coordinate in a two-link body experiencing free-fall (constrained by conservation of angular momentum). Raibert [11] introduced a pitch stabilization mechanism relying on reaction torques from hip actuation during stance. In this paper, we adopt the approach of composing these templates for 2DOF stabilization of appropriately defined "pitch" and "shape" coordinates of a two-link body/tail model.

Keeping in mind that in the physical system the tail actuator, τ_2, is unavailable for attitude control in stance (because it is being "monopolized" as the destabilizing energy source for the SLIP subsystem), and that the Raibert pitch correction mechanism (inserted through the hip actuator, τ_1) is unavailable in flight (due to absence of ground reaction force), we present a hybrid inertial reorientation (HIR) template (Fig. 6) as the simplest exemplar body on which this 2DOF template is anchored.

We omit the Lagrangian derivation for this familiar subsystem [10], but exploit the fact that when pinned at the CoM, the dynamics are second-order LTI with no Coriolis terms. We perform a change of coordinates (inverting the constant inertia tensor) to obtain the (decoupled) dynamics

$$\begin{bmatrix} \ddot{a}_1 \\ \ddot{a}_2 \end{bmatrix} = \begin{cases} \begin{bmatrix} \tau_1 \\ \delta \end{bmatrix} & =: p_1^{\mathsf{a}}(Ta, \tau_1) \quad \text{(stance)}, \\ \begin{bmatrix} 0 \\ \tau_2 \end{bmatrix} & =: p_2^{\mathsf{a}}(Ta, \tau_2) \quad \text{(flight)}, \end{cases} \tag{13}$$

where (a_1, a_2) are the "pitch" and "shape" coordinates, respectively, and δ is an unmodeled disturbance term (explicitly added here with an eye toward the use of tail for spring energization in the physical system). In (13) we have now represented HIR as two *independent* subsystems on which two identical 1DOF templates will be anchored in parallel (albeit in alternating stages of the hybrid execution).

Taking advantage of the direct affordance (by which we mean that both of the two decoupled 1DOF systems are completely actuated in, one and then other, of the alternating modes of their hybrid dynamics), we employ a graph-error controller [27] as a type of reduction. Since our reference first-order dynamics are just $\dot{a}_i = -ka_i$, the independent closed-loop 1DOF subtemplate vector fields, $f^{\mathsf{p}} : Ta_1 \mapsto \dot{Ta}_1$ and $f^{\mathsf{sh}} : Ta_2 \mapsto \dot{Ta}_2$, are defined as

$$\ddot{a}_i = -k_g(\dot{a}_i + ka_i) = -k_g k a_i - k_g \dot{a}_i, \tag{14}$$

where the gain k_g is understood to be high enough to make the transients of the anchoring dynamics irrelevant.

A. Hybrid Dynamical Model of HIR

Since the isolated model does not have any intrinsic physical mechanism for transitioning between modes, we add an exogenous clock signal, $\psi_a \in S^1$ such that $\psi_a \in [0, \pi]$ represents stance, and the complement represents flight.

Define $\mathcal{D}^{\mathsf{a}} = TS^2 \times \{(0, \pi] \sqcup (\pi, 2\pi]\}$. Now the closed-loop template dynamics, $f^{\mathsf{a}} : TS^2 \times S^1 \to T(TS^2 \times S^1)$ can be specified as

$$\begin{aligned} f_1^{\mathsf{a}}(\begin{bmatrix} Ta \\ \psi_a \end{bmatrix}) &= \begin{bmatrix} \begin{bmatrix} 0 & & & \\ -k_g k & 0 & -k & 0 \\ 0 & 0 & 0 & 0 \\ & & 0 & \end{bmatrix} & \begin{bmatrix} I & 0 \\ 0 & 0 \\ 0 & \omega_a \end{bmatrix} \\ 0 & 0 \end{bmatrix} \begin{bmatrix} Ta \\ \psi_a \end{bmatrix} + \begin{bmatrix} 0_{3\times 1} \\ \delta \\ 0 \end{bmatrix}, \\ f_2^{\mathsf{a}}(\begin{bmatrix} Ta \\ \psi_a \end{bmatrix}) &= \begin{bmatrix} \begin{bmatrix} 0 & & & \\ 0 & -k_g k & 0 & -k \\ 0 & 0 & 0 & 0 \\ & & 0 & \end{bmatrix} & \begin{bmatrix} I & 0 \\ 0 & 0 \\ 0 & \omega_a \end{bmatrix} \\ 0 & 0 \end{bmatrix} \begin{bmatrix} Ta \\ \psi_a \end{bmatrix}, \end{aligned} \tag{15}$$

the guards sets are $\partial\mathcal{D}^{\mathsf{a}} = TS^2 \times \{\{\pi\} \sqcup \{2\pi\}\}$ and the reset maps $r_i^{\mathsf{a}} = \mathrm{id}$ simply modify the dynamics (13) at $\psi_a = \pi$ (stance to flight) and $\psi_a = 0$ (flight to stance).

B. HIR Stability Analysis

Let us denote $\bar{\delta}[i] := \int \delta dt$, the interval being over the stance phase of stride i. Also, define $\bar{\delta}_{\max} = \max_t \bar{\delta}[t]$.

Proposition 6 (HIR Stability)**.** *Setting*

$$k > \frac{2\omega_a}{\pi} \log\left(1 + \frac{\bar{\delta}_{\max}}{\varepsilon_a}\right)$$

results in the desired limiting behavior for F^{a}: $\|a\| \to \mathcal{B}_{\varepsilon_a}(0)$, a neighborhood of 0 of size ε_a.

Proof. Please see Appendix H. □

[11] Formally, this means that k_p can be chosen as a function of ε_{r}.

V. Physical System: Tailed Monoped

We were able to formally show template-anchor relations going from 1DOF to 2DOF templates (Propositions 5 and 6), because of the availability of simple models (§III-B.2), or trivial dynamics (§IV). However, as we proceed up the desired hierarchy (Fig. 2), there are no easily accessible tools that let us directly analyze the effects of coupling in the return map. In this section, we only show (Proposition 8) that under assumption 4, the closed-loop tailed monoped return map F^{tm} has an invariant submanifold where it is equal to $F^{\mathsf{s}} \times F^{\mathsf{a}}$, but we leave as conjecture that this invariant submanifold is attracting.

A. The Tailed Monoped Model

The Raibert planar hopper [11] empirically demonstrated stable hopping using a rigid body with a massless springy leg, and in this paper we pursue the same idea, but instantiate the Raibert vertical hopping template by coupling the 1-DOF leg-spring excitation controller (physically acting through the tail). In flight, the tail actuator grants us a new affordance that we only[12] use here to regulate the added "shape" DOF.

Our physical model is shown in Fig. 2 (center). The system has a single massless leg with joints $\theta = (\theta_1, \theta_2) \in S^1 \times \mathbb{R}_+$, a rigid body $(x, z, \phi_1) \in \mathrm{SE}(2)$, and a point-mass tail with revolute DOF ϕ_2, such that the full configuration is $\mathbf{q} := (\theta_1, \theta_2, x, z, \phi_1, \phi_2) \in \mathcal{Q}$.

We make the following design-time assumptions:

Assumption 4 (Tailed monoped design)**.** *The (i) leg/tail axes of rotation are coincident at the "hip," (ii) center of mass (configuration-independent by the previous assumption) coincides with the hip, (iii) the tail mass is small, i.e. $m_t \ll m_b$, and (iv) the body, tail have high inertia, i.e. $i_b, i_t \to \infty$.*[13]

B. "Physical" Decoupling

We show from the equations of motion (cf. Appendix I) that the design choices in assumption 4 contribute to a natural (weak) decoupling of the 6DOF dynamics into "point-mass" and attitude compartments.[14]

Proposition 7 (Invariant submanifold)**.** *Under assumption 4, in each hybrid mode, (i) the submanifold $\mathcal{U} = \{T\mathbf{q} \in T\mathcal{Q} : T\phi_1 = T\phi_2 = 0\}$ is invariant under the action of the flow generated by f_i^{tm}, and (ii) in each hybrid mode, the closed-loop flow restricted to $\mathcal{U}$, $\dot{T\mathbf{q}} = f_i^{\mathsf{tm}}(T\mathbf{q}\,|_{\mathcal{U}})$ is a cross-product of the template vector fields,*

$$f_i^{\mathsf{tm}} = f_i^{\mathsf{s}} \circ \pi_s \times f_i^{\mathsf{a}} \circ \pi_a, \tag{16}$$

[12]We omit a detailed design discussion here, but a revolute tail avoids the morphological specialization of a dedicated prismatic actuator and can be repurposed for other uses such as static standing, reorienting the body in free fall [10], directing reaction forces through ground contact for leaping when used as another "leg" [28], etc.

[13]Even though the dynamic task here is quite different from free-fall, in the language of [10] this is saying that the tail should be light but *effective*.

[14]Considering that many running multilegged animals act SLIP-like [3], this kind of result can be interpreted to mean that the dynamics of the complicated running body may be a simple cross product of the template (SLIP) dynamics and the body-specific anchoring dynamics [7].

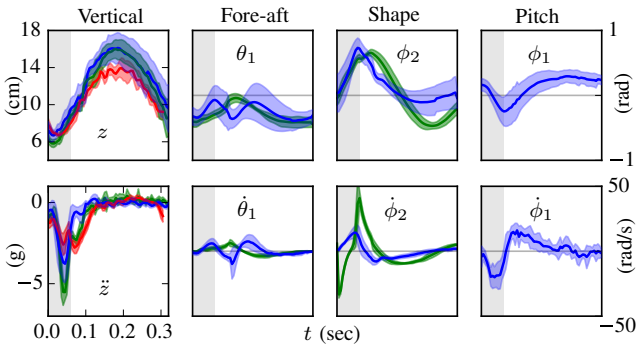

Fig. 7. A single stride (stance with shaded background followed by flight), where each column corresponds to some representative time series from each of the four 1DOF templates from §III-IV, and the traces (mean and standard deviation) correspond to different "bodies" realized by variably constraining the robot—**red:** tailed vertical hopper (i.e. (θ_1, x, ϕ_1) locked), **green:** tailed point-mass hopper (i.e. ϕ_1 locked), **blue:** tailed planar hopper (all free)—in which these templates are being anchored.

where π_s and π_a represent projections to the SLIP and attitude components of $\mathbf{q}$ respectively (cf. Appendix I).

Proof. Please see Appendix J. □

The statement above unfortunately does not guarantee anything about the limiting behavior of the hybrid physical system in a neighborhood of (the zero measure set) $\mathcal{U}$. We leave the missing piece as a conjecture, and present experimental evidence that it is indeed true in §VI:

Conjecture 2. *(Attracting invariant submanifold) The set $\mathcal{U}$ is attracting under the action of f^{tm}.*

C. Parallel Composition of Hybrid Templates

Building on Proposition 7 and Conjecture 2, we can now make the following statement:

Proposition 8 (Clock synchronization and TM return map)**.** *The set $\mathcal{U}$ is invariant under the return map $F^{\mathsf{tm}}(T\mathbf{q}\,|_{\mathcal{U}})$, and restricted to $\mathcal{U}$, $F^{\mathsf{tm}} = F^{\mathsf{s}} \circ \pi_s \times F^{\mathsf{a}} \circ \pi_a$.*

Proof. Please see Appendix K. □

VI. Experimental Results

We perform the experiments on the Penn Jerboa: a new tailed bipedal robot platform (Fig. 1) with a pair of compliant hip-actuated legs (in parallel for sagittal plane behaviors), and a 2DOF revolute point-mass tail [10] driven differentially by two motors through a five-bar mechanism (locked in the sagittal plane for the behaviors in this paper). The robot weighs 2 Kg (with onboard battery), has a peak robot power density of 300 W/Kg, and peak force density of 52.7 N-m/Kg. An IMU and motor encoders comprise the sensing capabilities (without payloads), and control is performed on an onboard Cortex-M4F microcontroller.

By physically constraining some of the degrees of freedom, we test the efficacy of our hierarchical composition (Fig. 2) at as many "nodes" of the composition tree as possible. Note that it is infeasible to isolate the fore-aft or the closed-loop pitch correction templates in a physical

setting. The results are summarized in Fig. 7. Five strides are averaged within each category, and aligned with ground truth knowledge of the touchdown event. We observe that with the same controllers acting in each case,

i) there is a limit cycle in the vertical compartment that retains its rough profile and magnitude through three anchoring bodies,
ii) the fore-aft DOF (hip angle) roughly satisfies $\ddot{\theta}_1 = 0$ in stance and the time of stance is roughly constant (corroborating assumptions 3.ii-iii) and corroborating our MBHop model (8),
iii) the shape coordinate is destabilized in stance and stabilized in flight, and the pitch-deflections seem relatively small in magnitude over the stride, and in agreement with (15).

Qualitatively, the "tailed point-mass hopper" configuration attained stable forward hopping at controlled speeds upwards of 20 strides, only limited by space. The fully unlocked system has so far hopped for about 10 strides at multiple instances before failing due to accumulated error causing large deviations from the limit cycle. We believe the prime reason for this is that in the hardware platform, the CoM is significantly aft of the hip (violating assumption 4.i). We attempted to compensate for this effect with a counterbalance visible in Fig. 1, but an unacceptably large weight would have been required to completely correct the problem.

VII. Discussion

Raibert's hopper [11] made significant empirical advances in the field of robotics, but to our knowledge, no previous account in the literature has provided any formal conditions under which such simple and decoupled control strategies will work. In this paper, we apply simple decoupled controllers using similar ideas (including the exact same fore-aft (7) and pitch (15) controllers), but with a new vertical hopping scheme (§III-A) and a new tail appendage to enable it. Moreover, we construct abstract models (that appear to, nevertheless, be representative of empirical data) that enable us to present analyses of stability for each of these subsystems, culminating in a local proof of stability for the tailed hopper (§V-C) and also essentially including an account of the Raibert hopper's empirical success.

Our analysis in this paper is very specifically targetted to the tailed hopper (including the hand-designed hierarchy in Fig. 2), but in future work we plan to generalize these ideas to other tasks as well as platforms. As explained in §II, we focus on closed-loop templates in this paper, but there is an accompanying interesting problem of assignment of actuator affordances to the control of specific compartments.

Lastly, we see in this paper that a sufficient condition for enabling a simple parallel composition is a physical decoupling (§V-B) through the design (summarized in Assumption 4) and natural dynamics of the system. In the future we wish to leverage recent advances in self-manipulation [25] to enable a direct analysis of the system dynamics, perhaps even enabling tools for designing machines based on a desired composition hierarchy (Fig. 2).

References

[1] E. Westervelt and J. Grizzle, *Feedback Control of Dynamic Bipedal Robot Locomotion*, ser. Control and Automation Series. CRC PressINC, 2007.

[2] R. Tedrake, "Underactuated robotics: Learning, planning, and control for efficient and agile machines course notes for MIT 6.832," Tech. Rep., 2009.

[3] P. Holmes, R. J. Full, D. Koditschek, and J. Guckenheimer, "The dynamics of legged locomotion: Models, analyses, and challenges," *Siam Review*, vol. 48, no. 2, pp. 207–304, 2006.

[4] M. Buehler, D. Koditschek, and P. Kindlmann, *A simple juggling robot: Theory and experimentation*, ser. Lecture Lecture Notes in Control and Information Sciences, 1989, vol. 139, p. 3573.

[5] L. L. Whitcomb, A. A. Rizzi, and D. E. Koditschek, "Comparative experiments with a new adaptive controller for robot arms," *Robotics and Automation, IEEE Transactions on*, vol. 9, no. 1, pp. 59–70, 1993.

[6] S. A. Burden, S. Revzen, S. S. Sastry, and D. E. Koditschek, "Event-selected vector field discontinuities yield piecewise-differentiable flows," *arXiv:1407.1775 [math]*, Jul 2014, arXiv: 1407.1775.

[7] R. J. Full and D. E. Koditschek, "Templates and anchors: neuromechanical hypotheses of legged locomotion on land," *Journal of Experimental Biology*, vol. 202, no. 23, pp. 3325–3332, Dec. 1999.

[8] R. Blickhan and R. J. Full, "Similarity in multilegged locomotion: Bouncing like a monopode," *Journal of Comparative Physiology A: Sensory, Neural, and Behavioral Physiology*, vol. 173, no. 5, p. 509517, 1993.

[9] T. Libby, T. Y. Moore, E. Chang-Siu, D. Li, D. J. Cohen, A. Jusufi, and R. J. Full, "Tail-assisted pitch control in lizards, robots and dinosaurs," *Nature*, vol. 481, no. 7380, pp. 181–184, Jan. 2012.

[10] A. M. Johnson, E. Chang-Siu, T. Libby, M. Tomizuka, R. J. Full, and D. E. Koditschek, "Tail assisted dynamic self righting," in *Proceedings of the Intl. Conf. on Climbing and Walking Robots*, 2012.

[11] M. Raibert, *Legged Robots that Balance*, ser. Artificial Intelligence. MIT Press, 1986.

[12] G. B. Gillis, L. A. Bonvini, and D. J. Irschick, "Losing stability: tail loss and jumping in the arboreal lizard anolis carolinensis," *Journal of Experimental Biology*, vol. 212, no. 5, pp. 604–609, Mar. 2009.

[13] T. E. Higham, M. S. Davenport, and B. C. Jayne, "Maneuvering in an arboreal habitat: the effects of turning angle on the locomotion of three sympatric ecomorphs of anolis lizards," *Journal of Experimental Biology*, vol. 204, no. 23, pp. 4141–4155, Dec. 2001.

[14] A. O. Pullin, N. J. Kohut, D. Zarrouk, and R. S. Fearing, "Dynamic turning of 13 cm robot comparing tail and differential drive," in *Robotics and Automation (ICRA), 2012 IEEE International Conference on*. IEEE, 2012, pp. 5086–5093.

[15] S. M. O'Connor, T. J. Dawson, R. Kram, and J. M. Donelan, "The kangaroo's tail propels and powers pentapedal locomotion," *Biology Letters*, vol. 10, no. 7, pp. 20 140 381–20 140 381, July 2014.

[16] G. Secer and U. Saranl, "Control of monopedal running through tunable damping." IEEE, Apr. 2013, pp. 1–4.

[17] O. Arslan and U. Saranli, "Reactive planning and control of planar spring-mass running on rough terrain," *IEEE Transactions on Robotics*, vol. 28, no. 3, pp. 567–579, June 2012.

[18] E. Eriksson, "Compartment models and reservoir theory," *Annual Review of Ecology and Systematics*, pp. 67–84, 1971.

[19] S. Burden, S. Revzen, and S. S. Sastry, "Dimension reduction near periodic orbits of hybrid systems," in *Decision and Control and European Control Conference (CDC-ECC), 2011 50th IEEE Conference on*. IEEE, 2011, pp. 6116–6121.

[20] D. E. Koditschek and M. Buehler, "Analysis of a simplified hopping robot," *The International Journal of Robotics Research*, vol. 10, no. 6, pp. 587–605, Dec. 1991.

[21] R. M. Ghigliazza, R. Altendorfer, P. Holmes, and D. Koditschek, "A simply stabilized running model," *SIAM Review*, vol. 47, no. 3, pp. 519–549, Jan. 2005.

[22] J. Pratt, J. Carff, S. Drakunov, and A. Goswami, "Capture point: A step toward humanoid push recovery," in *Humanoid Robots, 2006 6th IEEE-RAS International Conference on*. IEEE, 2006, pp. 200–207.

[23] S. Kajita, F. Kanehiro, K. Kaneko, K. Fujiwara, K. Harada, K. Yokoi, and H. Hirukawa, "Biped walking pattern generation by using preview control of zero-moment point," in *IEEE International Conference on Robotics and Automation, 2003. Proceedings. ICRA '03*, vol. 2, Sept. 2003, pp. 1620–1626 vol.2.

[24] W. J. Schwind and D. E. Koditschek, "Control of forward velocity for a simplified planar hopping robot," in *Robotics and Automation, 1995. Proceedings., 1995 IEEE International Conference on*, vol. 1, 1995, pp. 691–696.
[25] A. M. Johnson and D. E. Koditschek, "Legged self-manipulation," *IEEE Access*, vol. 1, pp. 310–334, May 2013.
[26] J. Schmitt and P. Holmes, "Mechanical models for insect locomotion: dynamics and stability in the horizontal plane i. theory," *Biological cybernetics*, vol. 83, no. 6, pp. 501–515, Dec. 2000.
[27] D. E. Koditschek, "Adaptive techniques for mechanical systems," in *Proc. 5th. Yale Workshop on Adaptive Systems*, May 1987, p. 259265.
[28] A. M. Johnson and D. E. Koditschek, "Toward a vocabulary of legged leaping," in *Proc. ICRA 2013*, May 2013, pp. 2553–2560.
[29] J. Guckenheimer and P. Holmes, *Nonlinear Oscillations, Dynamical Systems, and Bifurcations of Vector Fields*, ser. Applied Mathematical Sciences. Springer New York, 2013.

APPENDIX

A. Oscillatory Energization Stability Proof (Proposition 1)

First, note that other than $x = 0$, there are no fixed points for our parameter regime, $\omega > \sigma$. (It can be checked that two more equilibria appear otherwise.)

We can find a trapping region, $\mathcal{R}_o := \{x : \|x\| \leqslant \frac{k_t}{\sigma}\}$ (shown in Fig. 3). To see why, note that

$$x^T f_1^{\mathsf{v}}(x) \leqslant -\sigma x^T x + \frac{k_t x^T x}{\|x\|}, \tag{17}$$

i.e. $\|x\| \geqslant \frac{k_t}{\sigma} \implies \frac{d}{dt}(x^T x) \leqslant 0$.

Next, note that

$$Df_1^{\mathsf{v}} \mid_{x=0} = \begin{bmatrix} (-1+\frac{k_t}{\varepsilon})\sigma & (1+\frac{k_t}{\varepsilon})\omega \\ -\omega & -\sigma \end{bmatrix}, \tag{18}$$

for which $\operatorname{tr} Df_1^{\mathsf{v}} \mid_{x=0} = \sigma \cdot (\frac{k_t}{\varepsilon} - 2) > 0$ for a sufficiently small ε, and $\det Df_1^{\mathsf{v}} \mid_{x=0} = 1 + \frac{k_t}{\varepsilon}(\omega^2 - \sigma^2) > 0$, by assumption. Thus, $x = 0$ is a source.

Now we know that the trapping region is annular, and contains no equilibria. Applying the Poincare-Bendixson Theorem [29], we conclude that the limiting trajectory is a closed orbit lying inside the trapping region.

B. Vertical Stance Map (§III-A)

Writing $x(t, x_0)$ to denote the flow generated by (1), and letting $\mathcal{S}(x_0) := \min\{t > 0 \mid \pi_1 x(t, x_0) = 0\}$ denote the stance time (since π_1, the projection onto the position component, vanishes exactly at the liftoff), we define the vertical stance map, $F_1^{\mathsf{v}}(\dot\chi) := \pi_2 x(\mathcal{S}(\dot\chi, 0), (\dot\chi, 0))$.

C. Raibert Speed Controller Stability Proof (Proposition 3)

Note that

$$\begin{aligned} D_{\dot x}(\dot x^+ - \dot x) &= D_\beta(\dot x^+ - \dot x) \cdot D_{\dot x}\beta(\dot x) \\ &= D_\beta(\dot x^+ - \dot x) \cdot (D_{\dot x}\beta^* + k_p) \\ \implies D_{\dot x}\dot x^+ \mid_{\dot x = \dot x^*} &= 1 + D_\beta(\dot x^+ - \dot x) \cdot (D_{\dot x}\beta^* + k_p). \end{aligned}$$

From the sign properties of various terms, we note that for small k_p, $-1 < D_{\dot x}\dot x^+ < 1$.

TABLE III
PHYSICAL PARAMETERS (ALL SCALARS UNLESS NOTED)

k_t	Tail gain (3)
k_p	Raibert speed controller gain (7)
k	Inertial reorientation generalized damper gains (14)
k_g	Inertial reorientation graph error gain (14)
σ, ω	Dissipation, frequency of spring-damper (§III-A)
ε	Saturation parameter for tail controller (3))
ε_r	Stability margin for vertical hopping (Proposition 5)
ε_a	Arbitrarily small orientation error (Proposition 6)
m_b, i_b	Mass, inertia of robot body (§V)
ρ_l, ρ_t	Leg, tail link lengths (§III,V)
k_s	Hooke's law leg spring constant (§III,V)

D. Fore-aft Stability Proof (Proposition 4)

We can check that F^{fa} satisfies each of the Raibert conditions (Fig. 5), thereby concluding automatically from Proposition 3 that the Raibert controller will ensure local stability.

Alternatively, the utility of our simple analytical model (8)-(9) is that we can directly compute the stability properties under the Raibert controller (7),

$$DF^{\mathsf{fa}}(v) := \mathrm{R} + J\mathrm{R}v \cdot (D\gamma - 2D\beta)e_1^T, \tag{19}$$

where R is evaluated at $\gamma - 2\beta$. By inspection, the (desired) fixed point of (9) is $\beta = \gamma/2$ (this is the neutral touchdown angle). Evaluated at the fixed point,

$$DF^{\mathsf{fa}}(v^*) = I - 2k_p J v^* e_1^T = \begin{bmatrix} 1+2k_p v_2^* & 0 \\ -2k_p v_1^* & 1 \end{bmatrix}, \tag{20}$$

which is lower-triangular. The eigenvalues are $\{1, 1+2k_p v_2^*\}$, which capture the local stability of the single fore-aft DOF ($1 + 2k_p v_2 < 1$) as well as the degeneracy of the map.

To see why the last statement is true, note that we can find a rank 1 map

$$\iota : \mathbb{R}^2 \to \mathbb{R} : v \mapsto \|v\|,$$

which is invariant to F^{fa}, i.e. $\iota \equiv \iota \circ F^{\mathsf{fa}}$. Taking a gradient of both sides and using the chain rule,

$$D\iota \mid_v = D\iota \mid_{F^{\mathsf{fa}}(v)} \cdot DF^{\mathsf{fa}} \mid_v .$$

Evaluating at the fixed point v^*,

$$D\iota \mid_{v^*} = D\iota \mid_{v^*} \cdot DF^{\mathsf{fa}} \mid_{v^*},$$

i.e. $D\iota \mid_{v^*}$ is a left eigenvector of $DF^{\mathsf{fa}} \mid_{v^*}$ with unity eigenvalue.

Consequently, under iterations of this map, we get an invariant submanifold spanned by the orthogonal complement of the unity eigenvector, resulting in a "dimension reduction" (to a codimension 1 submanifold). In our case, F^{fa} is really a 1D map, even though its (co)domain in $\mathbb{R}^2$.

E. Hybrid Dynamical Model of SLIP (§III-C.1)

1) The Guard Set is $\partial\mathcal{D}^{\mathsf{s}}$: Since $\mathcal{Q}^{\mathsf{s}}$ is itself a cross product of Euclidean spaces and Lie groups, we can identify the tangent bundle with a cross product, $T\mathcal{Q}_i^{\mathsf{s}} \approx \mathcal{Q}_i^{\mathsf{s}} \times \mathbb{R}^4$. Then, the boundary of the product space only contains parts from $\mathcal{I}_i$, which corresponds exactly to the zeros of $\mathbf{a}^{\mathsf{s}}$ (§III-C.1).

2) Reset Maps: Let us define the functions

$$\mathrm{Cart} : S^1 \times \mathbb{R}_+ \to \mathbb{R}^2 : \left[\begin{smallmatrix}\theta_1\\ \theta_2\end{smallmatrix}\right] \mapsto \theta_2 \left[\begin{smallmatrix}-\sin\theta_1\\ \cos\theta_1\end{smallmatrix}\right] \tag{21}$$

$$\mathrm{Pol} : \mathbb{R}^2 \to S^1 \times \mathbb{R}_+ : u \mapsto \begin{bmatrix}\angle u\\ \|u\|\end{bmatrix}. \tag{22}$$

The reset maps are defined as

$$r_1^{\mathsf{s}} : \mathcal{D}^{\mathsf{s}} \to \mathcal{D}^{\mathsf{s}} : \begin{bmatrix}\theta\\ \dot\theta\\ \left[\begin{smallmatrix}x\\ z\end{smallmatrix}\right]\\ \left[\begin{smallmatrix}\dot x\\ \dot z\end{smallmatrix}\right]\end{bmatrix} \mapsto \begin{bmatrix}\theta\\ \dot\theta\\ \mathrm{Cart}(\theta)\\ D\mathrm{Cart}|_\theta\cdot\dot\theta\end{bmatrix}$$

$$r_2^{\mathsf{s}} : \mathcal{D}^{\mathsf{s}} \to \mathcal{D}^{\mathsf{s}} : \begin{bmatrix}\theta\\ \dot\theta\\ \left[\begin{smallmatrix}x\\ z\end{smallmatrix}\right]\\ \left[\begin{smallmatrix}\dot x\\ \dot z\end{smallmatrix}\right]\end{bmatrix} \mapsto \begin{bmatrix}\mathrm{Pol}(\left[\begin{smallmatrix}x\\ z\end{smallmatrix}\right])\\ D\mathrm{Pol}\cdot\left[\begin{smallmatrix}\dot x\\ \dot z\end{smallmatrix}\right]\\ \left[\begin{smallmatrix}-z\tan\beta(\dot x)\\ z\end{smallmatrix}\right]\\ \left[\begin{smallmatrix}\dot x\\ \dot z\end{smallmatrix}\right]\end{bmatrix}$$

F. Diffeomorphism to Leg-Polar Coordinates (§III-C.2)

Lemma 9. *Let* $\mathcal{V} := \{v \in \mathbb{R}^2 : v_2 < -\frac{2\rho_l}{T_s}\}$. *Then* $h_{\mathrm{w}} \mid_{\mathcal{V}}$ *is a local diffeomorphism.*[15]

Proof. Note that

$$Dh_{\mathrm{w}} = \mathrm{R} - J\mathrm{R}vD\beta e_1^T,$$

where R is understood to be evaluated at $-\beta(v)$. By inspection, Dh_{w} could only have a test vector $\mathrm{R}^T J\mathrm{R}v$ in its kernel, i.e.

$$Dh_{\mathrm{w}} \cdot (\mathrm{R}^T J\mathrm{R}v) = (1 - D\beta e_1^T \mathrm{R}^T J\mathrm{R}v)J\mathrm{R}v \neq 0,$$

since we know $v \neq 0$, $D\beta = \left(\frac{T_s}{2\rho_l} + k_p\right)$ and so

$$1 - D\beta e_1^T \mathrm{R}^T J\mathrm{R}v = 1 + v_2\left(\tfrac{T_s}{2\rho_l} + k_p\right) < 0,$$

by the conditions assumed on k_p. Thus Dh_{w} is nonsingular, and h_{w} is a local diffeo. □

G. Compositional Proof of SLIP Stability (Proposition 5)

We choose to perform our stability analysis at a section just after touchdown (in $w = h_{\mathrm{w}}(v)$ coordinates). From (8), the return map in w-coordinates is

$$\begin{aligned}\widetilde{F^{\mathsf{s}}}(w) &:= h_{\mathrm{w}} \circ F^{\mathsf{s}} \circ h_{\mathrm{w}}^{-1}(w) \mid_{\kappa = h_\kappa(w_2)}\\ &= \mathrm{R}(\eta(w))\left[\begin{smallmatrix}1\\ h_\kappa(w_2)\end{smallmatrix}\right] w,\end{aligned}$$

where $\eta := (\gamma - \beta - \beta \circ F^{\mathsf{s}}) \circ h_{\mathrm{w}}^{-1}$. Now,

$$D\widetilde{F^{\mathsf{s}}} = D_w\widetilde{F^{\mathsf{s}}} + D_\kappa\widetilde{F^{\mathsf{s}}} \cdot Dh_\kappa e_2^T,$$

where the first summand can be thought of as loosely the isolated fore-aft subsystem behavior, and the second summand is the perturbation from the radial subsystem. We will evaluate this quantity at the fixed point $w^* = h_{\mathrm{w}}(v^*)$.

Observe that using (7), $D\eta \mid_* = -2k_p e_1^T Dh_{\mathrm{w}}^{-1}$. Proceeding just like in Proposition 2,

$$\begin{aligned}Dh_\kappa \mid_* &= -\frac{1}{w_2^*}\left(1 + DF_1^{\mathrm{v}} \mid_{w_2^*}\right),\\ D_\kappa\widetilde{F^{\mathsf{s}}} = \mathrm{R}(\eta)e_2 e_2^T w &\implies D_\kappa\widetilde{F^{\mathsf{s}}} \mid_* = w_2^* e_2.\end{aligned}$$

[15]Physically, the restriction to $\mathcal{V}$ means that the hopper must have sufficient vertical component of touchdown velocity, essentially eliminating "grazing" ground impacts.

Lastly, the "isolated" term computes similar to (20),

$$\begin{aligned}D_w\widetilde{F^{\mathsf{s}}} &= \mathrm{R}\left[\begin{smallmatrix}1 & \kappa\end{smallmatrix}\right] + J\mathrm{R}\left[\begin{smallmatrix}1 & \kappa\end{smallmatrix}\right] wD\eta,\\ \implies D_w\widetilde{F^{\mathsf{s}}} \mid_* &= I + Jw^* D\eta \mid_*.\end{aligned}$$

Putting all of these together,

$$D\widetilde{F^{\mathsf{s}}} \mid_* = \left[\begin{smallmatrix}1\\ -DF_1^{\mathrm{v}}\mid_*\end{smallmatrix}\right] + pq^T,$$

where $p := -2k_p Jw^*, q^T := e_1^T Dh_{\mathrm{w}}^{-1}$. Using the matrix determinant lemma,

$$\begin{aligned}\mathrm{tr}\, D\widetilde{F^{\mathsf{s}}} &= 1 - DF_1^{\mathrm{v}} \mid_* + p^T q\\ \det D\widetilde{F^{\mathsf{s}}} &= -DF_1^{\mathrm{v}} \mid_* \left(1 - q^T\left[\begin{smallmatrix}1\\ -DF_1^{\mathrm{v}}\mid_*^{-1}\end{smallmatrix}\right] p\right).\end{aligned}$$

Now notice that since Dh_{w} is well-conditioned, we can claim an upper bound on

$$|p^T q| \leqslant 2k_p \|Jw^*\| \|Dh_{\mathrm{w}}^{-1}\| \leqslant k_p \Xi.$$

Also, the quadratic form $q^T\left[\begin{smallmatrix}1\\ -DF_1^{\mathrm{v}}\mid_*^{-1}\end{smallmatrix}\right] p$ must have

$$\left|q^T\left[\begin{smallmatrix}1\\ -DF_1^{\mathrm{v}}\mid_*^{-1}\end{smallmatrix}\right] p\right| \leqslant |p^T q|,$$

since $\left[\begin{smallmatrix}1\\ -DF_1^{\mathrm{v}}\mid_*^{-1}\end{smallmatrix}\right]$ has norm less than 1.

It can be checked that both eigenvalues are of absolute value bounded by unity iff all of (i) $\det < 1$, (ii) $\det > \mathrm{tr} - 1$, and (iii) $\det > -\mathrm{tr} - 1$ are true. These inequalities follow from condition (ii) of Proposition 5 and choosing small enough k_p such that $2k_p\Xi < \varepsilon_{\mathrm{r}}$.

H. Proof of HIR Stability (§IV-B)

Simply integrating the first-order dynamics (15), we get the touchdown return map $F^{\mathrm{a}} : S^2 \to S^2$,

$$F^{\mathrm{a}}(a) = \zeta \cdot \left(a + \bar\delta\left[\begin{smallmatrix}0\\ 1\end{smallmatrix}\right]\right), \tag{23}$$

where $\zeta := e^{-k\pi/\omega_a}(1 - k\pi/\omega_a)$. Iterating this return map, at stride $n \in \mathbb{Z}_+$,

$$a[n] = \zeta^t a[0] + (\zeta^n\bar\delta[0] + \cdots + \zeta\bar\delta[n-1])e_2, \tag{24}$$

and using the triangle inequality,

$$\|a[n]\| \leqslant |\zeta|^n \cdot \|a[0]\| + \bar\delta_{\max}\left|\tfrac{\zeta}{1-\zeta}\right|. \tag{25}$$

Note that $\zeta < \frac{1}{1+\bar\delta_{\max}/\varepsilon_a}$ is a sufficient condition to ensure that $\|a[t]\| \leqslant \varepsilon_a$ asymptotically stable. Some algebra reveals that

$$k > \tfrac{2\omega_a}{\pi}\log\left(1 + \tfrac{\bar\delta_{\max}}{\varepsilon_a}\right) \tag{26}$$

is, in turn, a condition sufficient to insure that previous inequality involving ζ.

I. Lagrangian Analysis of Tailed Monoped (§V-B)

We use the self-manipulation [25] formulation of hybrid dynamics. The inertia tensor is

$$\mathbf{M} = \begin{bmatrix} 0 & \\ & \mathbf{M}_b \end{bmatrix}, \text{ where } \mathbf{M}_b := \begin{bmatrix} \mathbf{M}_1 & \mathbf{M}_o^T \\ \mathbf{M}_o & \mathbf{M}_2 \end{bmatrix}. \tag{27}$$

Note that $\mathbf{M}_1 = (m_b + m_t)I$ and $\mathbf{M}_2 = \begin{bmatrix} i_b+i_t & i_t \\ i_t & i_t \end{bmatrix}$ are constant, and $\mathbf{M}_o$ contains the critical cross-compartment interaction, by way of which we can use our tail actuator (formally acting on an attitude DOF, ϕ_2) for energizing the shank DOF, θ_2.

Let the forward kinematics of the leg be $\mathbf{g} : \theta \mapsto \mathbb{R}^2$. The constraint in the stance contact mode is

$$\mathbf{a}_1(\mathbf{q}) = \begin{bmatrix} x \\ z \end{bmatrix} - \mathrm{R}(\phi_1)\mathbf{g}(\theta), \tag{28}$$

such that $\mathbf{A}_1(\mathbf{q}) = \begin{bmatrix} \mathrm{R}D\mathbf{g} & I & J\mathrm{R}\mathbf{g} & 0 \end{bmatrix}$. In flight mode, $\mathbf{a}_2(q) \equiv 0$. As in [25], the dynamics can be expressed as

$$\begin{bmatrix} \mathbf{M} & \mathbf{A}_i^T \\ \mathbf{A}_i & 0 \end{bmatrix} \begin{bmatrix} \ddot{\mathbf{q}} \\ \lambda \end{bmatrix} = \begin{bmatrix} \Upsilon - \mathbf{N} \\ 0 \end{bmatrix} - \begin{bmatrix} \mathbf{C} \\ \dot{\mathbf{A}}_i \end{bmatrix} \dot{\mathbf{q}}. \tag{29}$$

Define the linear coordinate change $\mathbf{h} : \mathcal{Y} = \mathcal{S} \times \mathcal{A} \to \mathcal{Q}$, and $\mathbf{H} := D\mathbf{h}$ such that

$$\mathbf{h}^{-1} : \mathbf{q} \mapsto \begin{bmatrix} (\theta_1+\phi_1, \theta_2, x, z)^T \\ \mathbf{M}_2 \begin{bmatrix} \phi_1 \\ \phi_2 \end{bmatrix} \end{bmatrix}, \tag{30}$$

and observe that $\mathbf{h}^{-1}(\mathbf{q}) = (s, a)$ is reminiscent of SLIP (§III) and attitude (§IV) coordinates. Define

$$\pi_s := \begin{bmatrix} I_4 & 0 \end{bmatrix} \mathbf{h}^{-1}, \qquad \pi_a := \begin{bmatrix} 0 & I_2 \end{bmatrix} \mathbf{h}^{-1} \tag{31}$$

The equations of motion are generated in the new coordinates,

$$\ddot{\mathbf{y}} = \mathbf{H}^{-1}\mathbf{M}^\dagger(\Upsilon - \mathbf{N}) - \mathbf{H}^{-1}(\mathbf{M}^\dagger\mathbf{C} + \mathbf{A}^{\dagger T}\dot{\mathbf{A}})\mathbf{H}\dot{\mathbf{y}}. \tag{32}$$

In stance,

$$\begin{bmatrix} \ddot{s}_1 \\ \ddot{s}_2 \end{bmatrix} = \begin{bmatrix} \frac{\tau_h}{m_b \theta_2^2} - \frac{2\dot{\theta}_2 \dot{\theta}_s}{\theta_2} \\ \frac{k_s(\rho_l - \theta_2)}{m_b} + \theta_2 \dot{\theta}_s^2 \end{bmatrix} + \frac{\tau_t}{\rho_t m_b} \begin{bmatrix} \sin\xi/\theta_2 \\ -\cos\xi \end{bmatrix}, \tag{33}$$

$$\ddot{a} = \begin{bmatrix} -\tau_h \\ \tau_t \end{bmatrix}, \tag{34}$$

where $\xi := \theta_1 - \phi_2$ (the tail-leg angle), and the right summand in (33) is quite clearly the disturbance caused due to the added attitude degrees of freedom.

With the same choice of $\mathbf{H}$, we can similarly recover weakly decoupled flight dynamics:

$$\begin{bmatrix} \ddot{x} \\ \ddot{z} \end{bmatrix} = \begin{bmatrix} 0 \\ -g \end{bmatrix} + \frac{\tau_t}{\rho_t m_b} \begin{bmatrix} \sin(\phi_1+\phi_2) \\ -\cos(\phi_1+\phi_2) \end{bmatrix}, \tag{35}$$

$$\ddot{a} = \begin{bmatrix} 0 \\ \tau_t \end{bmatrix}, \tag{36}$$

J. Tailed Monoped Flow Invariance (Proposition 7)

Applying assumption 4.iii to the Lagrangian analysis of Appendix I, the plant dynamics $p^{\mathsf{tm}}(T\mathbf{q}, (\tau_h, \tau_t))$ are

$$\begin{aligned} \ddot{\theta} \,|_{\text{stance}} &= \begin{bmatrix} \frac{\tau_h}{m_b \theta_2^2} - \frac{2\dot{\theta}_2 \dot{\theta}_s}{\theta_2} \\ \frac{k_s(\rho_l - \theta_2)}{m_b} + \theta_2 \dot{\theta}_s^2 \end{bmatrix} + \frac{\tau_t}{\rho_t m_b} \begin{bmatrix} \sin\xi/\theta_2 \\ -\cos\xi \end{bmatrix}, \\ \ddot{a} \,|_{\text{stance}} &= \begin{bmatrix} -\tau_h \\ \tau_t \end{bmatrix}, \\ \begin{bmatrix} \ddot{x} \\ \ddot{z} \end{bmatrix} |_{\text{flight}} &= \begin{bmatrix} 0 \\ -g \end{bmatrix} + \frac{\tau_t}{\rho_t m_b} \begin{bmatrix} \sin(\phi_1+\phi_2) \\ -\cos(\phi_1+\phi_2) \end{bmatrix}, \\ \ddot{a} \,|_{\text{flight}} &= \begin{bmatrix} 0 \\ \tau_t \end{bmatrix}, \end{aligned} \tag{37}$$

We can check that we have available affordances through our two actuators to assign (scaled versions of) our template controllers in Table II, (i) $\tau_h \,|_{\text{stance}} = -g_1^{\mathsf{p}}(a_1, \dot{a}_1)$ to control a_1, and $\tau_h \,|_{\text{flight}} = g_2^{\mathsf{fa}}(\dot{x})$ to control $\dot{x}$, and (ii) $\tau_t \,|_{\text{flight}} = g_2^{\mathsf{sh}}(a_2, \dot{a}_2)$ to control a_2, and $\tau_t \,|_{\text{stance}} = -\rho_t \theta_2 m_b \cdot g_1^{\mathsf{v}}(\dot{z})$ to control hopping height[16].

Under assumptions 3.iv and 4.iv, we show that the highlighted terms in (37) vanish inside $\mathcal{U}$:

i) $\mathbf{M}_2 \to \infty$, so in the dynamics equations $\ddot{a} = 0$. Restricted to $\mathcal{U}$, $a \equiv 0$. This proves part (i) of the claim.
ii) From $\ddot{a} \equiv 0$ and (14), $\tau_h \,|_{\text{stance}} = \tau_t \,|_{\text{flight}} = 0$.
iii) Since $\phi_2 = 0$, $\xi = -\phi_1 \approx 0$ (from assumption 3.iv).

By comparing the thus-restricted plant dynamics (37) to (10), (11) and (13), we obtain part (ii) of the result.

K. Tailed Monoped Return Map Invariance (Proposition 8)

We first define the return map F^{tm} by instantiating a "cross-product" hybrid system $(\mathcal{D}^{\mathsf{tm}}, f^{\mathsf{tm}}, r^{\mathsf{tm}})$ as (a) $\mathcal{D}^{\mathsf{tm}} := \mathcal{D}^{\mathsf{s}} \times \widetilde{\mathcal{D}^{\mathsf{a}}}$, (b) $r^{\mathsf{tm}} := r^{\mathsf{s}} \times \widetilde{r^{\mathsf{a}}}$, and (c) f^{tm} as defined in Proposition 7, where $\widetilde{\mathcal{D}_i^{\mathsf{a}}} := TS^2 \times S^1$ for each i (ensuring $\partial\widetilde{\mathcal{D}^{\mathsf{a}}} = \varnothing$) and $\widetilde{r_i^{\mathsf{a}}} : \widetilde{\mathcal{D}_i^{\mathsf{a}}} \to \widetilde{\mathcal{D}_{i+1}^{\mathsf{a}}}$ is defined

$$\widetilde{r_i^{\mathsf{a}}} : \begin{bmatrix} Ta \\ \psi_a \end{bmatrix} \mapsto \begin{bmatrix} Ta \\ i\pi \bmod 2\pi \end{bmatrix}. \tag{38}$$

With these modifications, the ψ_a dynamics (15) are ignored, and the clock of the HIR subsystem is being driven by the SLIP subsystem[17]. This ensures that the conditions of Proposition 6 still hold, i.e. $\pi_a \circ F^{\mathsf{tm}} = F^{\mathsf{a}} \circ \pi_a$.

Additionally, the decoupled nature of $f^{\mathsf{tm}} \,|_{\mathcal{U}}$ (Proposition 7) allows us to conclude that $\pi_s \circ F^{\mathsf{tm}} = F^{\mathsf{s}} \circ \pi_s$, so that

$$F^{\mathsf{tm}} = \pi_s \circ F^{\mathsf{tm}} \times \pi_a \circ F^{\mathsf{tm}} = F^{\mathsf{s}} \circ \pi_s \times F^{\mathsf{a}} \circ \pi_a,$$

which concludes the proof.

[16] We observe that by assumption 3.ii, $\theta_2 \approx \rho_l$ is roughly constant, so the scaling need not be configuration dependent.

[17] This coupling interaction importantly invalidates the ω_a-dependent bound on k (26). Our solution is to scale the input such that k is high enough for the shortest feasible transition time in vertical hopping.